haematologica
Journal of the Ferrata Storti Foundation

ICOS/ICOSL coexpression in Sézary syndrome reveals a potential tumor-promoting T-cell interaction

by Loubna Oumeslakht, Saskia Ingen-Housz-Oro, Amandine Decroos, Adèle De Masson, Caroline Ram-Wolff, Armand Bensussan, Emmanuele Lechapt, Rachid El Fatimy, Jérôme Giustiniani, Sanae Ben Mkaddem and Nicolas Ortonne

Received: August 14, 2026.
Accepted: November 6, 2026.

Citation: Loubna Oumeslakht, Saskia Ingen-Housz-Oro, Amandine Decroos, Adèle De Masson, Caroline Ram-Wolff, Armand Bensussan, Emmanuele Lechapt, Rachid El Fatimy, Jérôme Giustiniani, Sanae Ben Mkaddem and Nicolas Ortonne. ICOS/ICOSL coexpression in Sézary syndrome reveals a potential tumor-promoting T-cell interaction.
Haematologica. 2026 Nov 12. doi: 10.3324/haematol.2026.301825 [Epub ahead of print]

Publisher's Disclaimer.
E-publishing ahead of print is increasingly important for the rapid dissemination of science. Haematologica is, therefore, E-publishing PDF files of an early version of manuscripts that have completed a regular peer review and have been accepted for publication.
E-publishing of this PDF file has been approved by the authors.
After having E-published Ahead of Print, manuscripts will then undergo technical and English editing, typesetting, proof correction and be presented for the authors' final approval, the final version of the manuscript will then appear in a regular issue of the journal.
All legal disclaimers that apply to the journal also pertain to this production process.

ICOS/ICOSL coexpression in Sézary syndrome reveals a potential tumor-promoting T-cell interaction

Loubna Oumeslakht [1,2,3], Saskia Ingen-Housz-Oro[4], Amandine Decroos[2], Adèle de Masson[5,6]

, Caroline Ram-Wolff[5], Armand Bensussan[6,7], Emmanuele Lechapt[2,3,8], Rachid El Fatimy[1],

Jérôme Giustiniani [2,3#], Sanae Ben Mkaddem[1,#] and Nicolas Ortonne[2,3,8,#]

[1]Faculty of Medical Sciences, UM6P Hospitals, University Mohammed VI Polytechnic,

Benguerir, 43150, Morocco;

[2]IMRB (INSERM U955) Team Models and Oncogenesis of T-cell lymphomas (MOON-LYT), Créteil, F-94000, France;

[3]Université Paris Est Créteil, Créteil, France;

[4]APHP, Hôpital Henri Mondor, Dermatology Department, Créteil, F-94000, France;

[5]AP-HP, Saint Louis Hospital, Dermatology Department, Paris, France;

[6]Institut de Recherche Saint Louis, INSERM U1342, Hôpital Saint Louis, Paris, France;

[7]Institut Godinot, CLCC de Reims, 51100 Reims, France;

[8]AP-HP, Hôpital Henri Mondor, Pathology Department, Créteil, F-94000, France

[#]: These authors contributed equally to this work.

Corresponding authors:
Nicolas Ortonne
Department of Pathology, Assistance Publique - Hôpitaux de Paris,
Henri Mondor hospital, 1 rue Gustave Eiffel, 94000, Créteil, France.
Phone: +33149812738
Fax: +33149812733
E-mail: nicolas.ortonne@aphp.fr

And **Sanae Ben Mkaddem**
Faculty of Medical Sciences, UM6P Hospitals, University Mohammed VI Polytechnic, Benguerir, 43150, Morocco.
Phone: +212666931429
E-mail: sanae.benmkaddem@um6p.ma

Author's contributions: Conceptualization, Methodology, Investigation, data curation: LO,

SO, AD, ADM, CRW, AB, JG, SB, NO; Writing original draft: LO; Writing and editing: LO, EL, REF, SB, NO, AB; Project administration: NO, SB.

Data-sharing statement: Data are available upon request to authors (nicolas.ortonne@aphp.fr).

Acknowledgments: This work was supported by a grant from the French Society of Dermatology (Société Française de Dermatologie, SFD) and LO received a PhD grant from UM6P University and OCP Foundation. Our acknowledgments go to Dr. Susanne Melchers, Dr. Edyta Biskup and Dr. Laurence Michel for providing Seax cell lines, and Dr. Hélène Le-Buanec for providing the plasma samples of inflammatory diseases.

Conflict of interest statement: The authors declare no conflicts of interest.

AI use declaration: ChatGPT (Open AI) and DeepL were used for language proofreading to check grammar, spelling, and linguistic accuracy. The authors reviewed the suggested corrections and take full responsibility for the final content of the manuscript.

Main text

Sézary syndrome (SS) is a rare, aggressive, and clinically heterogeneous lymphoproliferative disorder characterized by the clonal expansion of malignant $CD4^+$ T-helper cells infiltrating the skin, lymph nodes, and peripheral blood.[1] Previously classified among cutaneous T-cell lymphomas (CTCL), SS has recently been reclassified by the World Health Organization as a mature T-cell and NK-cell leukemia.[1] Neoplastic Sézary cells (SC) typically display a $CD3^+$ $CD4^+$ $CD7^-$ $CD26^-$ immunophenotype[2] and frequently exhibit aberrant expression of KIR3DL2.[3] Diagnosis relies on a combination of clinical, histopathological and molecular assessments, often leading to delayed diagnosis.[2] Current treatments range from immunomodulators to systemic chemotherapy and immunotherapy.[2] However, the disease aggressiveness, heterogeneity, poor prognosis, and frequent relapse make its management challenging. Allogeneic stem cell transplantation remains the only potentially curative treatment but is limited to selected patients due to risks of relapse and treatment-related morbidity and mortality.[4] These challenges highlight the need to better understand the molecular and immunological mechanisms driving SS progression and to identify novel therapeutic targets.

The ICOS-ICOSL (inducible T-cell costimulator and its ligand) axis is a key co-stimulatory pathway regulating T-cell activation, survival, and cytokine production. Previous studies have shown increased ICOS expression in advanced-stage CTCL, including SS.[5] Preclinical studies have shown that an ICOS-targeting antibody-drug conjugate efficiently depletes malignant cells.[5] However, because ICOS is also expressed by non-malignant $CD4^+$ and $CD8^+$ T cells, this strategy may result in unwanted immune depletion. Malignant SC are known to aberrantly coexpress receptors and their cognate ligands, such as OX40/OX40L,[6] CD137/CD137L[7] and PD-1/PD-L1/PD-L2.[8] We therefore investigated the expression of ICOSL and its functional role in SS. In this study, we found that SC coexpress ICOS and ICOSL, supporting a model in which their interaction may promote tumor cell survival through activation of the AKT signaling pathway. We identified distinct ICOSL isoforms, including the previously unreported isoform 4.2, which contains a duplicated proline-rich domain and may have distinct signaling properties. Furthermore, targeting ICOSL with a recombinant ICOS-Fc fusion protein induced selective killing of SC in antibody-dependent cell cytotoxicity (ADCC) assays.

To assess ICOSL expression, we analyzed peripheral blood mononuclear cells (PBMC) from SS patients (n=34) (**Supplementary Table 1**) and healthy donors (HD, n=20) using flow cytometry. Samples were prospectively collected or retrospectively retrieved from the cutaneous lymphoma collection in the Biological Resource Center of Henri Mondor Hospital, approved by a Western IRB (#2015-A01306-43) in accordance with the declaration

of Helsinki. SC were identified as $CD3^+$ $CD4^+$ $KIR3DL2^+$ lymphocytes[3]. We found that SC expressed not only ICOS but also its ligand, ICOSL, which was absent on T lymphocytes from HD (**Figure 1A**) as described in a recent study.[9] ICOSL expression was significantly higher in SC compared to T cells from HD (*P*<0.0001) (**Figure 1B**), studied at baseline and after activation with CD3-CD28 coated beads (data not shown). Additionally, this expression was detected in both $KIR3DL2^+$ and $KIR3DL2^-$ T cells (**Supplementary Figure 1A-C**). ICOSL was also detected in several SS cell lines (Seax, HH, H9 and Hut-78) (**Figure 1C**), but not in other CTCL or peripheral T-cell lymphoma cell lines, including mycosis fungoides (Myla), anaplastic large cell lymphoma (FEPD, Su-DHL-1), and hepatosplenic gamma-delta T cell lymphoma (DERL2) (**Supplementary Figure 1D**). However, these findings are based on cell-line models and do not exclude the possibility of ICOSL expression in primary tumor cells of these lymphomas. Additionally, cytoplasmic ICOSL expression was observed in primary cells obtained from angioimmunoblastic T-cell lymphoma patient-derived xenograft mice models that have been developed by Tari et al.[10] Furthermore, we measured soluble ICOSL (sICOSL) levels in plasma from a second cohort comprising SS patients, HD, and patients with inflammatory diseases, including prurigo nodularis, atopic dermatitis, and systemic lupus erythematosus. sICOSL levels were significantly elevated in SS patients (mean ~ 2ng/ml) compared to HD (<1ng/ml), with levels similar to those observed in other inflammatory diseases (**Figure 1D**).

ICOSL contributes to T-cell activation primarily through interaction with two key costimulatory receptors: ICOS and CD28.[11,12] At least four ICOSL isoforms have been reported, sharing the same extracellular domain but differing in their cytoplasmic tails. Isoform 1 is predominantly expressed in lymphoid tissues, isoform 2 is broadly expressed, isoform 3 is truncated, and the long isoform 4 contains an extended cytoplasmic tail.[13] However, their functional differences are poorly understood. To characterize ICOSL isoform expression in circulating SC from patients with SS, we performed western blot analysis. In addition to the 35-kDa isoform 2, two higher-molecular-weight isoforms were detected, corresponding to the expected 53-kDa ICOSL isoform 4 and an additional 60-kDa protein (**Figure 2A**). To further characterize these proteins, RT-PCR using primers targeting the cytoplasmic domain of ICOSL isoform 4 generated two products of approximately 280 bp and 400 bp (**Figure 2B**). Sanger sequencing identified the 280-bp product as the canonical cytoplasmic tail of ICOSL isoform 4, hereafter referred to as ICOSL isoform 4.1. The 400 bp product contained the complete ICOSL isoform 4 sequence together with a duplicated segment encoding a 40-amino acid proline-rich domain. This previously unrecognized variant, designated ICOSL isoform 4.2, may confer distinct signaling properties (**Figure 2C**). Expression of isoforms 4.1 and 4.2 varied across patients: some expressed only

isoform 4.1, others only isoform 4.2, whereas both isoforms were detected in the remaining cases. This interpatient heterogeneity raises the possibility that these variants fulfill distinct biological functions.

The ICOS/ICOSL axis regulates multiple aspects of T-cell function, including activation, cytokine production, and differentiation.[14] To investigate the pathophysiologic role of ICOSL in SS, we examined ICOS–ICOSL trans-interactions. Previous studies have shown that ICOSL is downregulated upon binding to ICOS.[15] Accordingly, ICOSL-expressing H9 cells were cocultured with Jurkat cells ($ICOSL^-$ $ICOS^+$ $CD28^+$) or Su-DHL-1 cells ($ICOSL^-$ $ICOS^+$ $CD28^-$) (**Figure 3A**). ICOSL expression in H9 cells decreased after coculture and was restored following ICOS blockade, confirming ICOS–ICOSL trans-interaction (**Figure 3B**). We then assessed downstream signaling pathways activated by ICOSL in SS cell lines (HH, H9 and Seax). Engagement of ICOSL increased phosphorylation of PKCγ, AKT, CREB and GSK3β, whereas the MAPK pathway was not affected (**Figure 3 C-D**). These findings suggest that ICOSL activates selective signaling pathways involved in cell survival and function in SC.

In light of all these results, we may hypothesize that the coexpression of receptor-ligands pairs, such as ICOSL and ICOS, could establish autocrine or paracrine signaling loops at the level of SC that may promote their survival. It is possible that these interactions explain why tumor cells in CTCL (SS and mycosis fungoides in particular) are often clustered together. This is well known in epidermal infiltrates (“Pautrier abscesses”). Furthermore, according to an in situ cellular proximity analysis conducted on 8 biopsies from SS patients compared to 12 controls (inflammatory erythrodermic diseases), SC (PD-1+) also tended to cluster in the dermal infiltrates of SS to a greater extent than T cells (CD3+) in the infiltrates of the controls (**Supplementary Figure 2**).

To evaluate the therapeutic potential of targeting ICOSL, we conducted functional assays using a recombinant ICOS-Fc fusion protein capable of binding all ICOSL isoforms and inducing ADCC through NK cell engagement by the human IgG1-Fc format of the construct. CFSE-labeled Hut-78 cells were cocultured with NK cells from HD at various effector-to-target (E:T) ratios and treated with 5 µg/mL of ICOS-Fc, or an IgG1 isotype control. Mogamulizumab (anti-CCR4) was used as a positive control. ICOS-Fc significantly increased tumor cell death compared to the isotype control (**Figure 3E**), thereby providing initial proof of concept that ICOSL could potentially represent a new therapeutic target in SS. Since ICOSL is also expressed by normal hematopoietic cells, particularly B lymphocytes, we also evaluated the effect of the construct on B lymphocytes from healthy donors. NK-cell-mediated cytotoxicity was found to be specific to SS cells, with no detectable effect on normal B cells (**Figure 3F**). This lack of cytotoxicity toward normal B cells may be related to their lower physiological

expression of ICOSL, compared with the higher levels observed in SS cell lines. Hence, targeting ICOSL through such a strategy could offer a favorable therapeutic index. Overall, these findings provide new insights into the role of ICOSL in the pathobiology of T-cell lymphomas and support the development of therapeutic strategies targeting the ICOS/ICOSL pathway, including ICOSL-directed approaches.

References

1. Melchers S, Albrecht JD, Kempf W, Nicolay JP. The fifth edition of the WHO-Classification - what is new for cutaneous lymphomas? J Dtsch Dermatol Ges. 2024;22(9):1254-1265.

2. Dummer R, Vermeer MH, Scarisbrick JJ, et al. Cutaneous T cell lymphoma. Nat Rev Dis Primers. 2021;7(1):61.

3. Ortonne N, Huet D, Gaudez C, et al. Significance of circulating T-cell clones in Sézary syndrome. Blood. 2006;107(10):4030-4038.

4. Latzka J, Assaf C, Bagot M, et al. EORTC consensus recommendations for the treatment of mycosis fungoides/Sézary syndrome - Update 2023. Eur J Cancer. 2023;195:113343.

5. Amatore F, Gorvel L, Olive D. Role of inducible co-stimulator (ICOS) in cancer immunotherapy. Expert Opin Biol Ther. 2020;20(2):141-150.

6. Kawana Y, Suga H, Kamijo H, Miyagaki T, Sugaya M, Sato S. Roles of OX40 and OX40 ligand in mycosis fungoides and Sézary syndrome. Int J Mol Sci. 2021;22(22):12576.

7. Kamijo H, Miyagaki T, Shishido-Takahashi N, et al. Aberrant CD137 ligand expression induced by GATA6 overexpression promotes tumor progression in cutaneous T-cell lymphoma. Blood. 2018;132(18):1922-1935.

8. Pileri A, Tabanelli V, Fuligni F, et al. PD-1 and PD-L1 expression in mycosis fungoides and Sézary syndrome. Ital J Dermatol Venerol. 2022;157(4):355-362.

9. Oka K, Miyagawa T, Morita H, et al. Inducible costimulator and its ligand promote proliferation and migration of tumor cells in cutaneous T-cell lymphoma. Int J Mol Sci. 2026;27(3):1408.

10. Tari Crochet G, Ari-Yuka S, Fischer A, et al. Induction of p53-mediated apoptosis by azacitidine in patient-derived xenograft follicular helper T-cell lymphoma model. Leukemia. 2025;39(7):1744-1755.

11. Wang S, Zhu G, Chapoval AI, et al. Costimulation of T cells by B7-H2, a B7-like molecule that binds ICOS. Blood. 2000;96(8):2808-2813.

12. Yao S, Zhu Y, Zhu G, et al. B7-H2 Is a Costimulatory Ligand for CD28 in Human. Immunity. 2011;34(5):729-740.

13. Ling V, Wu PW, Miyashiro JS, Marusic S, Finnerty HF, Collins M. Differential expression of inducible costimulator-ligand splice variants: lymphoid regulation of mouse GL50-B and human GL50 molecules. J Immunol. 2001;166(12):7300-7308.

14. Tafuri A, Shahinian A, Bladt F, et al. ICOS is essential for effective T-helper-cell responses. Nature. 2001;409(6816):105-109.

15. Watanabe M, Takagi Y, Kotani M, et al. Down-regulation of ICOS ligand by interaction with ICOS functions as a regulatory mechanism for immune responses1. J Immunol. 2008;180(8):5222-5234.

Figures

Figure 1. ICOS and ICOSL expression in Sézary syndrome. (A) Representative flow cytometry analysis of ICOS and ICOSL on $CD4^+$ $KIR3DL2^+$ and $CD4^+$ $KIR3DL2^-$ T cells from a patient with Sézary syndrome (SS) and a healthy donor (HD). Cells were stained with anti-CD3-FITC (clone OKT3), anti-CD4-BV510 (clone RPA-T4), anti-KIR3DL2-PE (clone REA970), anti-ICOS-APC (clone C398.4A), and anti-ICOSL-APC (clone MIH12) monoclonal antibodies. Data were acquired using an LSRFortessa flow cytometer and analyzed with FlowJo software. **(B)** ICOS and ICOSL expression on $CD4^+$ T cells from patients with SS and HD. Expression levels are presented as median fluorescence intensity (MFI) normalized to the corresponding isotype control and appeared higher in SS as compared to HD ($p<0,0005$ for ICOS and $p<0,0001$ for ICOSL). **(C)** ICOSL expression in SS cell lines, assessed by flow cytometry using an anti-ICOSL monoclonal antibody (clone MIH12). **(D)** Plasma levels of soluble ICOSL in HD and patients with SS, prurigo nodularis (PN), atopic dermatitis (AD), and systemic lupus erythematosus (SLE). Soluble ICOSL concentrations were determined using the Human B7-H2/ICOS Ligand ELISA Kit (EH40RB, Invitrogen), according to the manufacturer's instructions. Statistical significance: ns, not significant ($p > 0.05$); * $p < 0.05$; *** $p < 0.001$; **** $p < 0.0001$.

Figure 2. Identification of two ICOSL isoforms expressed in Sézary syndrome. (A) Western blot analysis of ICOSL expression in samples from patients with SS. ICOSL was detected using a rabbit anti-ICOSL monoclonal antibody (clone EPR6071, 1:1,000), followed by a goat anti-rabbit IgG-HRP secondary antibody (1:10,000). **(B)** RT-PCR analysis of ICOSL isoform 4 expression in SS patient samples and cell lines. The forward primer sequence was 5'-CAGAGAGACGAGTGCTAGACCC-3', and the reverse primer sequence was 5'-TTCCAGGAGCAACATAGATGTG-3'. *Asterisk indicates samples obtained from FACS-sorted $CD4^+$ $KIR3DL2^+$ Sézary cells. For samples with a $CD3^+CD4^+KIR3DL2^+$ population representing ≥ 90% of cells, further purification of the neoplastic population was not performed. **(C)** ICOSL transcripts have been separated from agarose gel electrophoresis and subjected to Sanger sequencing. The corresponding protein sequences are shown for ICOSL isoform 4.1 (left) and isoform 4.2 (right).

Figure 3. Functional characterization of ICOSL in Sézary syndrome (SS). (A) Expression of ICOSL and its receptors, ICOS and CD28, in the Sézary syndrome H9 cell line, the acute T-cell leukemia Jurkat cell line, and the anaplastic large-cell lymphoma Su-DHL-1 cell line, assessed by flow cytometry. **(B)** Regulation of ICOSL expression in H9 cells following coculture with Jurkat cells ($ICOS^+CD28^+$) or Su-DHL1 cells ($ICOS^+CD28^-$), used to assess ICOS/CD28-ICOSL trans-interactions, in the presence of an anti-ICOS blocking antibody (clone Medi-570)

or the corresponding isotype control. **(C)** Analysis of AKT (Ser473; clone A21001C), CREB1 (Ser133; clone A22026B), and GSK3-β (Ser9; clone A2101BC) phosphorylation in H9 cells following treatment with an anti-ICOSL antibody or the corresponding isotype control, assessed by flow cytometry after fixation and permeabilization. **(D)** Analysis of PKCγ (Thr514; clone D6Y3D), AKT (S473; clone D9E), MAPK (Thr202/Tyr204; clone 9101S) phosphorylation in the HH cell line following treatment with an anti-ICOSL antibody (clone RD136726) or the corresponding isotype control, assessed by Western blot. **(E)** Percentage of cell death among CFSE-labeled Hut-78 cells cocultured overnight with NK cells and treated with recombinant ICOS-Fc, anti-CCR4 monoclonal antibody (mogamulizumab) or the corresponding isotype control. NK cells were enriched from peripheral blood mononuclear cells (PBMC) obtained from healthy donors (HD) using untouched magnetic cell-sorting protocol (MojoSort Human NK Cell Isolation Kit). **(F)** Percentage of cell death among normal B cells cocultured overnight with NK cells and treated with recombinant ICOS-Fc, anti-CD20 monoclonal antibody (Rituximab), or the corresponding isotype control. B cells were enriched from PBMC obtained from HD using an untouched magnetic cell-sorting protocol (MojoSort Human Pan B Cell Isolation Kit). Cytotoxicity was calculated as follows: ADCC (%) = [% $CFSE^+VD^+$ cells / (% of $CFSE^+VD^+$ cells + % of $CFSE^+VD^-$ cells)] x 100. Statistical significance: ns, not significant; * $p < 0.05$; ** $p < 0.01$; *** $p < 0.001$; **** $p < 0.0001$. NT, non-treated; PKC, protein kinase C; CREB1, cAMP response element-binding protein 1; GSK3β, glycogen synthase kinase-3 beta.

Abbreviations

ADCC: Antibody-Dependent Cell Cytotoxicity

CCR4: C-C Chemokine Receptor Type 4

CFSE: Carboxyfluorescein Succinimidyl Ester

CREB: cAMP Response Element-Binding Protein

CTCL: cutaneous T-cell lymphomas

GSK3β: Glycogen Synthase Kinase 3 Beta

HD: healthy donors

ICOS: Inducible T-cell costimulator

ICOSL: Inducible T-cell costimulator ligand

KIR3DL2: Killer cell immunoglobulin-like receptor 3DL2

MAPK: Mitogen-Activated Protein Kinases

NK: Natural killer

PBMC: Peripheral Blood Mononuclear Cells

PD-1: Programmed Cell Death Protein 1

PD-L1/2: Programmed Cell Death Ligand 1/2

PKCγ: Protein Kinase C Gamma

RT-PCR: Reverse Transcription Polymerase Chain Reaction

SC: Sézary cells

sICOSL: soluble Inducible T-cell costimulator ligand

SS: Sézary syndrome

Figure 1

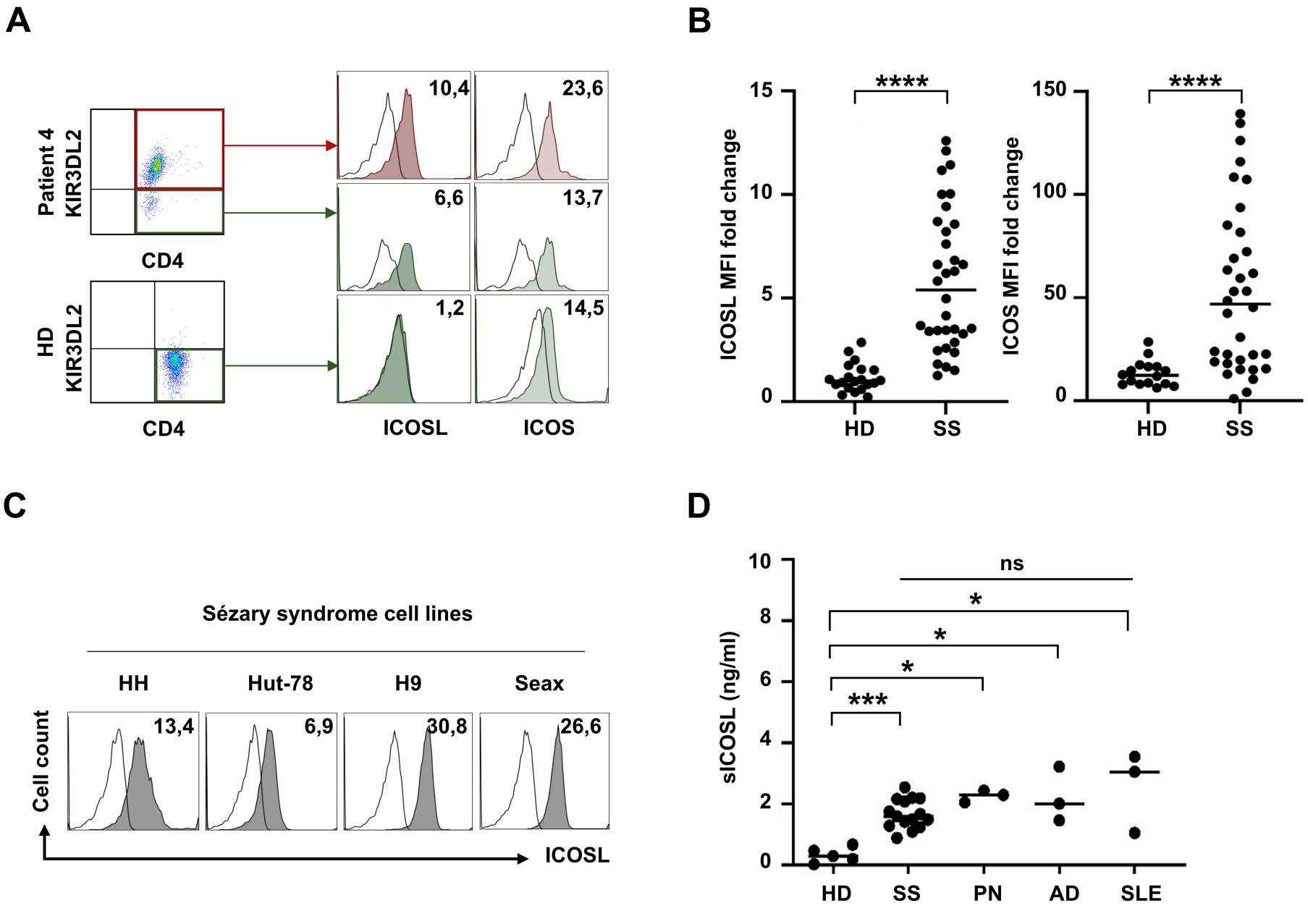
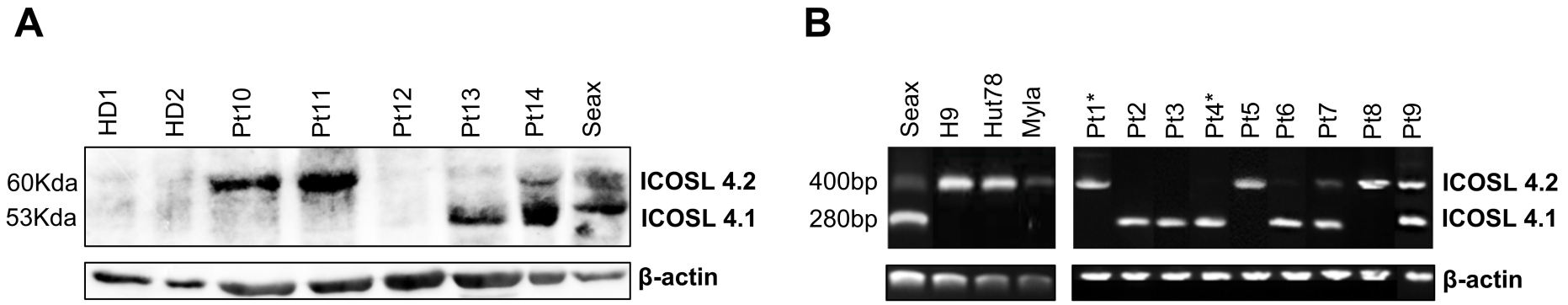

A
Patient 4
KIR3DL2
CD4
HD
KIR3DL2
CD4
10,4
23,6
6,6
13,7
1,2
14,5
ICOSL
ICOS
B
ICOSL MFI fold change
15
10
5
0
****
HD
SS
ICOS MFI fold change
150
100
50
0
****
HD
SS
C
Sézary syndrome cell lines
HH
Hut-78
H9
Seax
Cell count
13,4
6,9
30,8
26,6
ICOSL
D
sICOSL (ng/ml)
10
8
6
4
2
0
ns
*
*
*
***
HD
SS
PN
AD
SLE

Figure 2



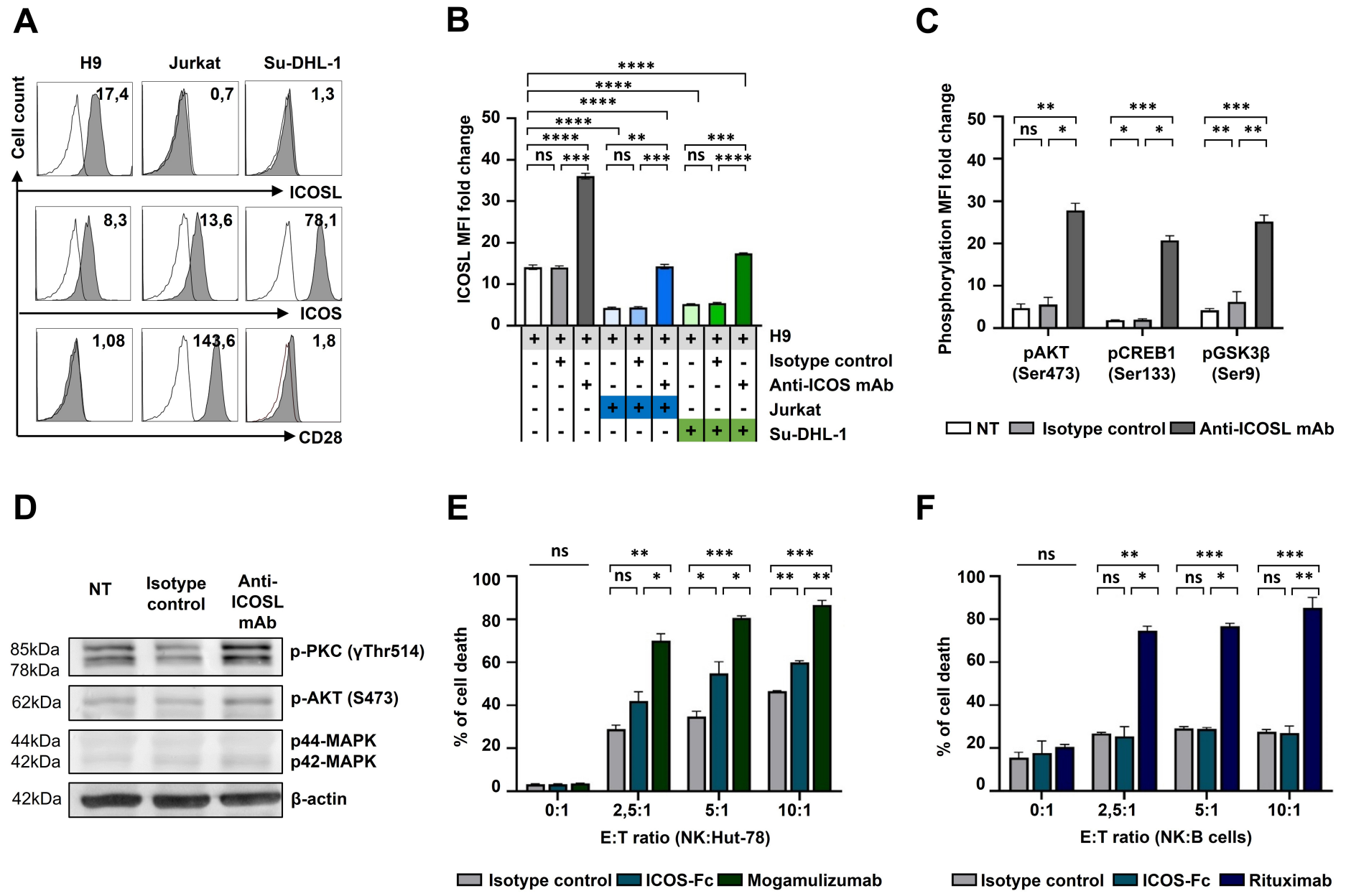
C




```
  1 MRLGSPGLLFLLFSSLRADTQEKEVRAMVGSDVELSCACPEGS
 44 RFDLNDVYVYWQTSESKTVVTYHIPQNSSLENVDSRYRNRALM
 87 SPAGMLRGDFSLRLFNVTPQDEQKFHCLVLSQSLGFQEVLSVE
130 VTLHVAANFSVPVVSAPHSPSQDELTFTCTSINGYPRPNVYWI
173 NKTDNSLLDQALQNDTVFLNMRGLYDVVSVLRIARTPSVNIGC
216 CIENVLLQQNLTVGSQTGNDIGERDKITENPVSTGEKNAATWS
259 ILAVLCLLVVVAVAIGWVCRDRCLQHSYAGAWAVSPETELTEE
302 FAVGSSRFWGAQGRLGCQLSFRVSKNFQKAKVPCLEQLLFLET
345 QRSPRWCAWHFLQPPLGMGWHPGVHFVTLRWDFPNMHRSRETS
388 ARPPRSPVPSPDQGVQGGSRHRRPAPMGCPEWVQAPAPSPRGV
431 SRAGPGTGAQPLWGVRSGSGHRQLLSVAATPAALVCPSVPGAT
```

```
  1 MRLGSPGLLFLLFSSLRADTQEKEVRAMVGSDVELSCACPEGS
 44 RFDLNDVYVYWQTSESKTVVTYHIPQNSSLENVDSRYRNRALM
 87 SPAGMLRGDFSLRLFNVTPQDEQKFHCLVLSQSLGFQEVLSVE
130 VTLHVAANFSVPVVSAPHSPSQDELTFTCTSINGYPRPNVYWI
173 NKTDNSLLDQALQNDTVFLNMRGLYDVVSVLRIARTPSVNIGC
216 CIENVLLQQNLTVGSQTGNDIGERDKITENPVSTGEKNAATWS
259 ILAVLCLLVVVAVAIGWVCRDRCLQHSYAGAWAVSPETELTEE
302 FAVGSSRFWGAQGRLGCQLSFRVSKNFQKAKVPCLEQLLFLET
345 QRSPRWCAWHFLQPPLGMGWHPGVHFVTLRWDFPNMHRSRETS
388 ARPPRSPVPSPDQGVQGGSRHRRPAPMGCPEWVQAPAPSPRGV
431 SRAGPGTGAQPPWGVQGGSRHRRPAPMGCPEWQAPAPSPRGVS
474 RAGPGTGAQPLWGVRSGSGHRQLLSVAATPAALVCPSVPGAT
```

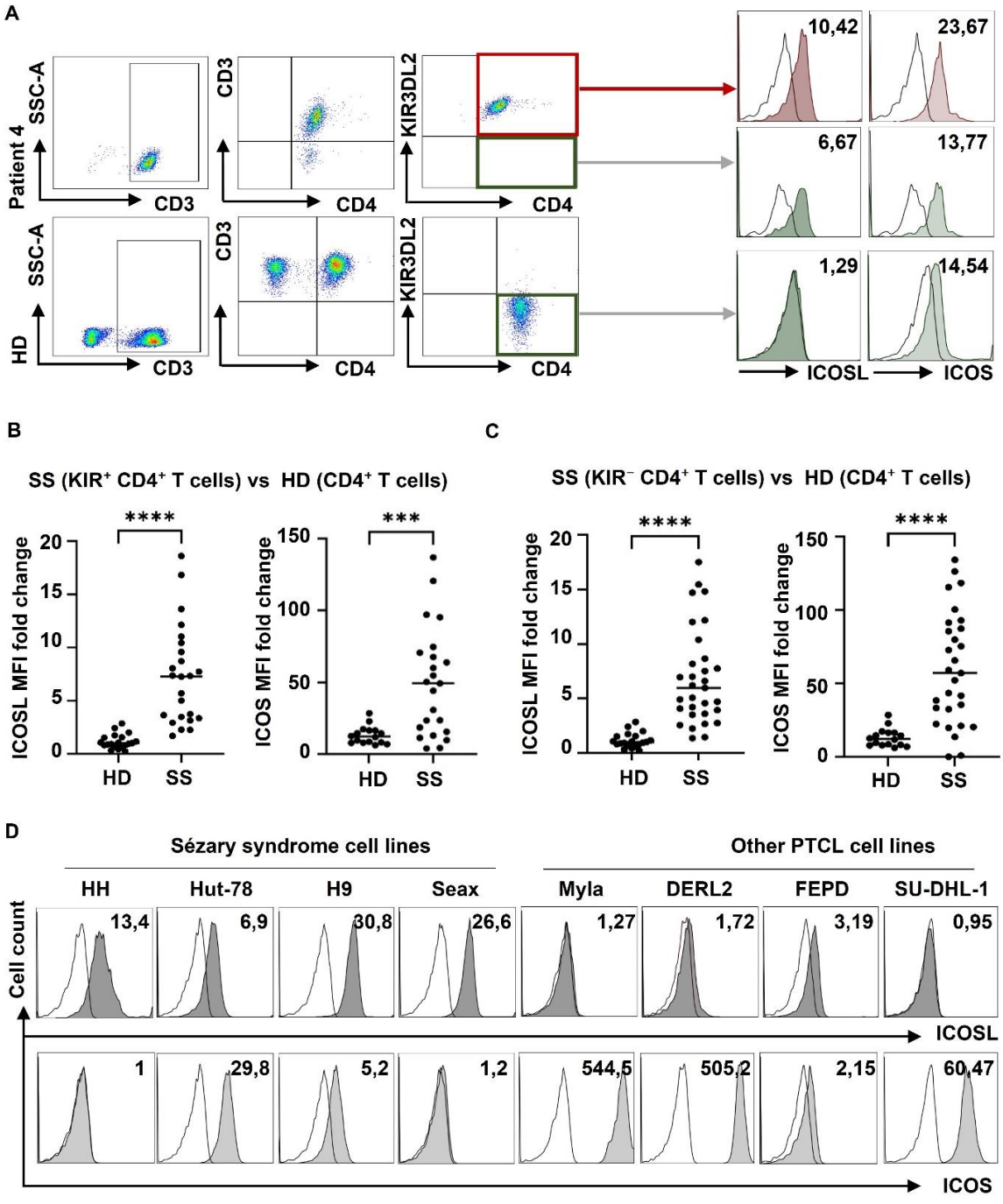
Figure 3


A
H9
Jurkat
Su-DHL-1
Cell count
17,4
0,7
1,3
ICOSL
8,3
13,6
78,1
ICOS
1,08
143,6
1,8
CD28
B
ICOSL MFI fold change
H9
Isotype control
Anti-ICOS mAb
Jurkat
Su-DHL-1
C
Phosphorylation MFI fold change
pAKT (Ser473)
pCREB1 (Ser133)
pGSK3β (Ser9)
NT
Isotype control
Anti-ICOSL mAb
D
NT
Isotype control
Anti-ICOSL mAb
85kDa
78kDa
p-PKC (γThr514)
62kDa
p-AKT (S473)
44kDa
42kDa
p44-MAPK
p42-MAPK
42kDa
β-actin
E
% of cell death
E:T ratio (NK:Hut-78)
Isotype control
ICOS-Fc
Mogamulizumab
F
% of cell death
E:T ratio (NK:B cells)
Isotype control
ICOS-Fc
Rituximab

ICOS/ICOSL coexpression in Sézary syndrome reveals a potential tumor-promoting T-cell interaction

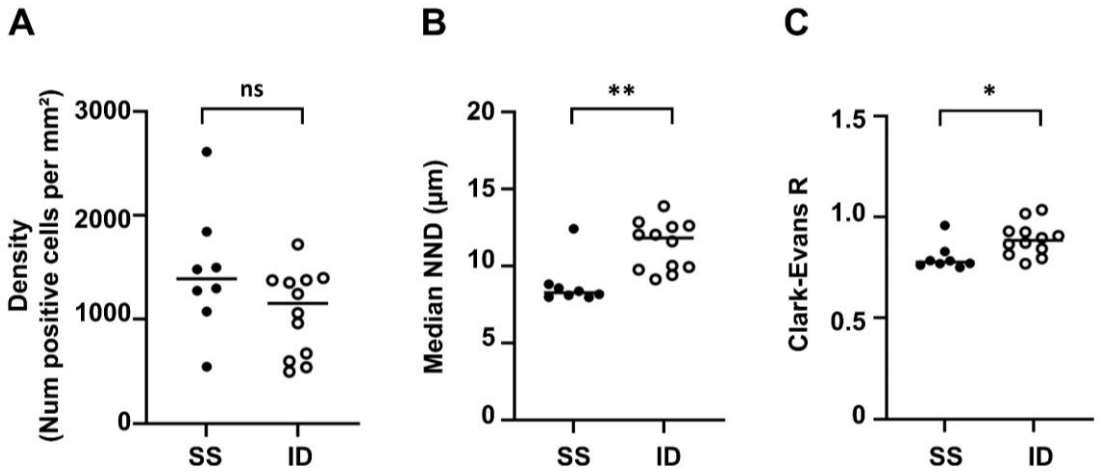
Supplementary data:

Supplementary Figure 1. ICOS and ICOSL expression in T-cell lymphomas. (A) Gating strategy for the analysis of ICOS and ICOSL expression in T cells from a representative patient with Sézary syndrome (SS) and a representative healthy donor (HD). **(B)** ICOS and ICOSL expression levels in KIR3DL2^{+}CD4^{+} T cells from patients with SS compared with CD4^{+} T cells from HDs. Expression levels appeared higher in SS as compared to HD ($p<0,0001$ for ICOS and $p<0,0001$ for ICOSL). Cells were stained with anti-CD3-FITC (clone OKT3), anti-CD4-BV510 (clone RPA-T4), anti-KIR3DL2-PE (clone REA970), anti-ICOS-APC (clone C398.4A), and anti-ICOSL-APC (clone MIH12) monoclonal antibodies. Data were acquired using an LSRFortessa flow cytometer and analyzed with FlowJo software **(C)** ICOS and ICOSL expression in KIR3DL2^{-}CD4^{+} T cells from patients with SS compared with CD4^{+} T cells from HD. Median fluorescence intensity (MFI) values were normalized to the corresponding isotype controls. Expression levels appeared higher in SS as compared to HD ($p<0,0001$ for ICOS and $p<0,0001$ for ICOSL). **(D)** ICOSL and ICOS expression in T-cell lymphoma cell lines including SS (SeAx, HH, HuT78, H9), mycosis fungoides (MyLa), hepatosplenic gamma-delta T-cell lymphoma (DERL-2), anaplastic large cell lymphoma (FEPD, SU-DHL-1).


A
Patient 4
HD
SSC-A
CD3
CD4
KIR3DL2
10,42
23,67
6,67
13,77
1,29
14,54
ICOSL
ICOS
B
SS (KIR+ CD4+ T cells) vs HD (CD4+ T cells)
ICOSL MFI fold change
ICOS MFI fold change
****
***
HD
SS
C
SS (KIR− CD4+ T cells) vs HD (CD4+ T cells)
D
Sézary syndrome cell lines
Other PTCL cell lines
HH
Hut-78
H9
Seax
Myla
DERL2
FEPD
SU-DHL-1
Cell count
13,4
6,9
30,8
26,6
1,27
1,72
3,19
0,95
1
29,8
5,2
1,2
544,5
505,2
2,15
60,47

Supplementary Figure 2: Spatial distribution and clustering analysis of Sézary cells compared with T cells from inflammatory erythrodermic diseases (ID). (A) Density of immunopositive cells (number of positive cells/mm²) in the SS and ID groups. **(B)** Median nearest neighbour distance (NND) of immunopositive cells. **(C)** Clark–Evans R index assessing the spatial organization of immunopositive cells. An R value < 1 indicates a clustered distribution, R = 1 indicates a random distribution, and R >1 indicates a dispersed distribution. Each dot represents an individual biopsy. Statistical significance: ns, no significant; p<0.05 (*); p<0.01 (**).

Eight skin biopsies from patients with SS and 12 biopsies from patients with inflammatory dermatoses, including atopic dermatitis (n=5), drug-induced dermatoses (Toxidermatoses, TOX) (n=2), psoriasis (n=5) were included. Tissue sections were stained for CD3 and PD-1 by Immunohistochemistry. Whole-slide images were analyzed using Qupath (version 0.5.1), with cell segmentation and detection of immunopositive cells were performed using the same software. The centroid coordinates (x, y) of immunopositive cells were exported for downstream spatial analyses in R (version 4.5.2). Spatial organization was assessed using NND and the Clark-Evans R index with the *spatstat.geom* package. The Euclidean distance between each cell and its nearest neighboring positive cell was calculated using the nndist() function, and the median NND was calculated for each biopsy as a summary measure of spatial organization. Clark-Evans R values <1, ≈1, and >1 indicate clustered, random, and dispersed distributions, respectively.



Supplementary Table 1: Clinical features of patients with Sézary syndrome.

Clinical characteristics	Values
Number of patients	41
Age, mean ± SD (years)	67.5 ± 15.1 [27-87]
Sex ratio, (men/women)	1/1
Clinical stage (n=24)	IB: 1 (4.2%); IIA: 1 (4.2%); IIB: 1 (4.2%); III: 1 (4.2%); IIIB: 1 (4.2%); IVA1: 10 (41.7%); IVA2: 9 (37.5%)
Treatment (n=26)	Untreated (2/41) Topical corticosteroids (2/41) Bexarotene (alone or in combination with ECP) (7/41) Methotrexate (1/41) Mogamulizumab (3/41) Lacutamab (2/41) Pembrolizumab (1/41) Romidepsine (2/41) Monochemotherapy (doxorubicin) (2/41) Polychemotherapy (4/41) Not reported (15/41)

Patients with Sézary syndrome (SS) were diagnosed in the Dermatology department of Henri Mondor hospital in France between 2021 and 2023. Peripheral blood samples were prospectively collected and sorted at the Henri Mondor Cutaneous Lymphoma Biobank. Peripheral blood samples from healthy donors (HD) were obtained from the Établissement Francais du Sang. ECP: extracorporeal photopheresis.